

# Kinetic and Scale-Up Investigations of Epoxide Aminolysis in Microreactors at High Temperatures and Pressures

Nikolay Zaborenko, Matthew W. Bedore, Timothy F. Jamison,\* and Klavs F. Jensen\*

Departments of Chemistry and Chemical Engineering, Massachusetts Institute of Technology, 77 Massachusetts Avenue, Cambridge, Massachusetts 02139, United States

## Abstract:

A continuous-flow microreactor is applied for a kinetic study of a model  $\beta$ -amino alcohol formation by epoxide aminolysis. A large number of experiments are performed in a short time with minimal reagent consumption. The kinetics of formation of secondary aminolysis between starting epoxide and product are decoupled from the primary synthesis, constructing a complete model for desired product formation. The activation energy for the formation of desired product is observed to be higher than those for regioisomer formation and for secondary aminolysis, indicating that increasing temperature improves selectivity in addition to accelerating the reaction. A set of optimized conditions is then selected for best reaction performance, and the process is scaled up to a 100-fold larger reactor volume with model predictions in good agreement with measured process performance.

## 1. Introduction

The synthesis of  $\beta$ -amino alcohols is an important pursuit in the pharmaceutical industry and in academic research. A number of active pharmaceutical ingredients (APIs), including Oxycontin, Coreg, and Toprol-XL, contain this moiety, while quite a few others, such as Zyvox and Skelaxin, feature oxazolidones that can be formed through  $\beta$ -amino alcohol precursors. Frequently, the precursors to  $\beta$ -amino alcohols are difficult to synthesize and/or very expensive; thus, being able to perform this reaction as rapidly and efficiently as possible with the highest possible yield is of great interest.

The  $\beta$ -amino alcohol functional group can be assembled by a number of synthetic pathways, with the most commonly reported among them being the ring-opening of epoxides with amine nucleophiles.<sup>1</sup> The epoxide functional group has long been a versatile functional group, able to produce a variety of compounds via different ring-opening reactions.<sup>2</sup> While epoxide aminolysis can, in most cases, be performed in the absence of a catalyst, it generally proceeds slowly when performed at typical temperatures of solvent reflux.

The use of elevated temperatures is one of the more general means of  $\beta$ -amino alcohol formation by the opening of epoxides with amines. Additionally, because of its inherent simplicity and lack of additional reagents and materials, it remains the preferred option for industrially practical syntheses due to the

ease of application. Elevating the reaction temperature is a commonly accepted method of reaction acceleration, typically limited principally by the stability of the reagents and/or the product. To achieve high temperatures, either high-boiling solvents are used, or the reaction is pressurized to increase the boiling point of the solvent. However, solvent properties have a very strong effect on the reaction rate;<sup>3</sup> therefore, it would be highly preferable to select an appropriate solvent based on its reaction properties and to enable the reaction to be performed at the highest temperature allowable by the stabilities of the chemical species.

While some work has been done using calorimetry for kinetic studies of epoxide aminolysis,<sup>4–6</sup> few reports have been published analyzing the kinetics and selectivities of this transformation in different solvents or applying kinetic results to process design.<sup>7</sup> Additionally, while there have been studies reporting the different kinetic parameters of primary and secondary amines acting as nucleophiles in the epoxide aminolysis,<sup>8–10</sup> we are unaware of reports investigating the rate of the  $\beta$ -amino alcohol product itself reacting with another molecule of epoxide (“bisalkylation”), generally an undesired process that decreases the yield of the overall desired reaction.

Microreactors for continuous-flow syntheses are becoming increasingly more popular in both academia and the pharmaceutical industry,<sup>11–14</sup> often used to more efficiently produce biologically active materials.<sup>15</sup> As compared to conventional batch processes, microsystems enable rapid heat and mass transfer, resulting in improved reaction profiles for more accurate kinetic studies. In addition to safely enabling high

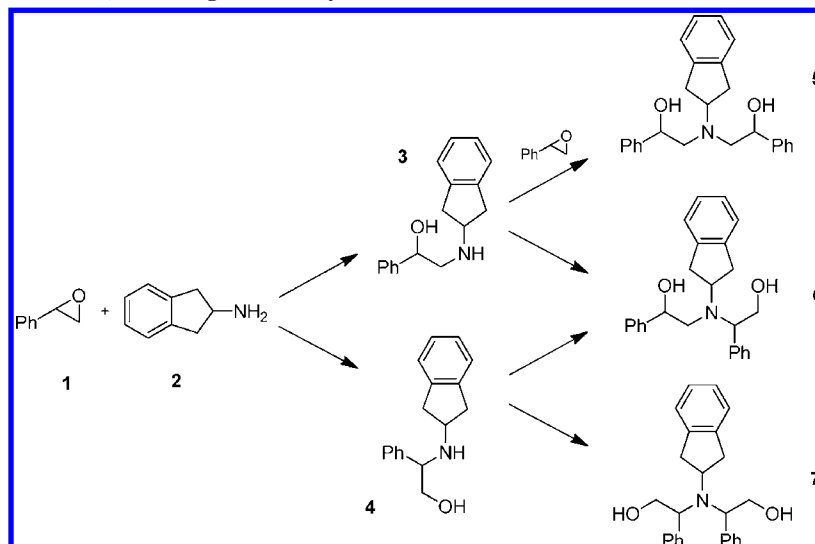
- (3) Kravchenko, V. V.; Kostenko, L. I.; Popov, A. F.; Kotenko, A. A.; Koblik, I. V. *Ukr. Chem. J.* **1990**, *56* (2), 168–172.
- (4) Vinnik, R. M.; Roznyatovsky, V. A. *J. Therm. Anal. Calorim.* **2003**, *73*, 807–817.
- (5) Vinnik, R. M.; Roznyatovsky, V. A. *J. Therm. Anal. Calorim.* **2003**, *73*, 819–826.
- (6) Vinnik, R. M.; Roznyatovsky, V. A. *J. Therm. Anal. Calorim.* **2004**, *75*, 753–764.
- (7) Sirovski, F.; Mulyashov, S.; Shvets, V. *Chem. Eng. J.* **2006**, *117* (3), 197–203.
- (8) Rogers, D. Z.; Bruce, T. C. *J. Am. Chem. Soc.* **1979**, *101* (16), 4713–4719.
- (9) Sundaram, P. K.; Sharma, M. M. *Bull. Chem. Soc. Jpn.* **1969**, *42* (11), 3141–3147.
- (10) Trejbal, J.; Petrisko, M. *React. Kinet. Catal. Lett.* **2004**, *82* (2), 339–346.
- (11) Jas, G.; Kirschning, A. *Chem.–Eur. J.* **2003**, *9* (23), 5708–5723.
- (12) Mason, B. P.; Price, K. E.; Steinbacher, J. L.; Bogdan, A. R.; McQuade, D. T. *Chem. Rev.* **2007**, *107* (6), 2300–2318.
- (13) Wiles, C.; Watts, P. *Expert Opin. Drug Discovery* **2007**, *2* (11), 1487–1503.
- (14) Wiles, C.; Watts, P. *Eur. J. Org. Chem.* **2008**, *2008* (10), 1655–1671.
- (15) Roberge, D. M.; Zimmermann, B.; Rainone, F.; Gottsponer, M.; Eyholzer, M.; Kockmann, N. *Org. Process Res. Dev.* **2008**, *12* (5), 905–910.

\* Authors to whom correspondence may be sent. E-mail: tfj@mit.edu; e-mail: kfjensen@mit.edu.

(1) Bergmeier, S. C. *Tetrahedron* **2000**, *56* (17), 2561–2576.

(2) Parker, R. E.; Isaacs, N. S. *Chem. Rev.* **1959**, *59* (4), 737–799.

**Scheme 1.** Aminolysis of **1** with **2**, including the bisalkylation reactions



temperatures and pressures not easily attainable in batch chemistry while allowing for rapid reaction monitoring,<sup>12</sup> microreactors are highly efficient in the use of reagents for kinetic screening studies.<sup>16,17</sup>

In our previous work,<sup>18</sup> we have demonstrated highly efficient aminolyses of epoxides using a continuous-flow silicon microreactor. Excellent yields and conversions with simple terminal epoxides were obtained at residence times under 5 min in ethanol under high temperature (180–240 °C) and pressure. Epoxide aminolysis in a continuous-flow microreactor was performed on pharmaceutically relevant syntheses (reaction steps towards metoprolol and indacaterol), accelerating the reactions by factors of 30–60 over the conventionally performed processes with similar product yields. The continuous-flow microreactor was also capable of reaching temperatures not easily attainable in typical batch processes, allowing for higher reaction temperatures, and due to the elimination of headspace, volatile amines and solvents could be used in the reaction without affecting reactant concentrations, allowing for kinetic studies.

To enable the determination of the optimal set of concentrations and conditions for performing epoxide aminolysis, a systematic evaluation of the kinetic parameters of the reaction is necessary. The aminolysis of styrene oxide **1** with 2-aminoindan **2**, as shown in Scheme 1, was selected for this study because the reagents are electronically similar to those participating in the epoxide aminolysis step in the formation of the pharmaceutical agent indacaterol.<sup>19</sup> The kinetic evaluation was performed using ethanol as the solvent, using very low concentrations of reagents to enable the measurement of initial reaction rates using short residence times and very low conversions. To fully determine the rate of formation of the

desired product **3**, the kinetics of the bisalkylation reaction (aminolysis of **1** with product **3** to form side product **5**) were first investigated. The determined reaction rate law of bisalkylation was then applied to decouple the kinetics of the primary reaction and to obtain the overall rate law of product **3** formation.

The knowledge imparted by the use of microreactors can then be applied, in conjunction with chemical engineering principles, to obtain efficient operating parameters on the industrial scale.<sup>20</sup> In this work, the kinetic model obtained in a given temperature range using dilute reagent solutions was extrapolated to higher temperatures and industrially relevant concentrations to demonstrate whether it is applicable in a broad range of conditions.

## 2. Results and Discussion

**2.1. Heat Transfer Analysis.** The high thermal conductivity of silicon (148 W/m·K compared to stainless steel ~40 W/m·K) greatly aids in spreading heat and significantly reduces the occurrence of hot spots. In the heated reactor zone, the compressed heating block, manufactured of aluminum and with graphite as the liner between the block and the reactor (see Experimental Section), further helped distribute the heat while providing high heat transfer. A two-dimensional lengthwise cross section of the reactor was simulated by finite element analysis, including the heating and compression chucks. A temperature of 455 K (182 °C) was assumed for the cartridge heaters, and a temperature of 285 K (12 °C) was given for the boundary between the compression piece and cooling fluid. The overall results of the simulation are shown in Figure 1.

It can readily be seen that the etched-out area of the reactor establishes thermal separation between the inlet/outlet area (including the mixing zone) and the reaction area of the reactor. This allows the area in contact with polymer o-rings and fittings to remain at room temperature when the compression chuck is water-cooled, while the reaction zone is at temperatures of up to 300 °C. Additionally, the temperature at the location of the

(16) Goodell, J. R.; McMullen, J. P.; Zaborenko, N.; Maloney, J. R.; Ho, C.-X.; Jensen, K. F.; Porco, J. A.; Beeler, A. B. *J. Org. Chem.* **2009**, *74* (16), 6169–6180.

(17) Murphy, E. R.; Martinelli, J. R.; Zaborenko, N.; Buchwald, S. L.; Jensen, K. F. *Angew. Chem., Int. Ed.* **2007**, *46* (10), 1734–1737.

(18) Bedore, M. W.; Zaborenko, N.; Jensen, K. F.; Jamison, T. F. *Org. Process Res. Dev.* **2010**, *14* (2), 432–440.

(19) Lohse, O.; Vogel, C. Process For Preparing 5-[(R)-2-(5,6-Diethylindian-2-ylamino)-1-hydroxy-ethyl]-8-hydroxy-(1H)-quinolin-2-one Salt, Useful As an Adrenoceptor Agonist. WO/2004/076422, 2004.

(20) Roberge, D. M.; Gottspomer, M.; Eyholler, M.; Kockmann, N. *Chem. Today* **2009**, *27* (4), 8–11.

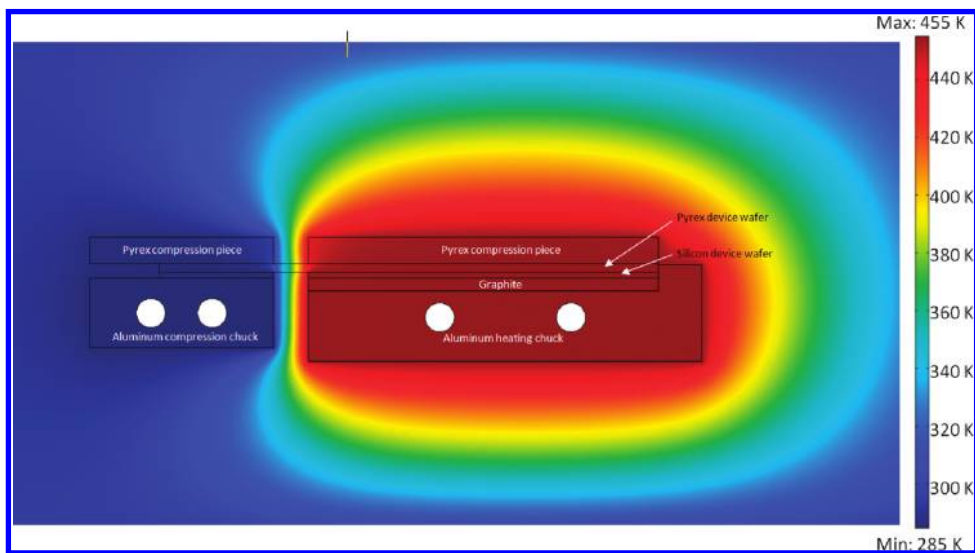


**Figure 1.** Finite element modeling of heat transfer in the reactor setup.

thermocouple is within 0.02 °C of that of the cartridge heaters. Furthermore, the maximum temperature variation across the reactive zone of the microreactor is <0.5 °C (see Figure S1 of Supporting Information). At the fastest flow rate used (360  $\mu\text{L}/\text{min}$ ), the fluid entering the reactive zone comes to within 1 °C of the desired temperature within 0.09 s, or 0.45% of the total residence time (see section S2 of Supporting Information for the derivation).

**2.2. Kinetic Evaluation of Bisalkylation.** Reaction kinetics were investigated and calculated on the basis of several assumptions regarding mixing within the microreactor channel. As flow within the microreactor was always very laminar (see section 2.4 for the discussion and Table 3 for the range of Reynolds numbers), no turbulence-driven macromixing could occur. Thus, the only effects to be considered were mixing by diffusion, axial dispersion, and Dean flow. On the basis of the small channel width, it was calculated that mixing by diffusion ensures that all incoming streams are fully mixed prior to entering the heated reaction zone. Additionally, the range of Péclet numbers in which the reactor was operated (also discussed in section 2.4 and Table 3) was such that axial dispersion could be considered negligible, justifying the assumption of plug flow. Therefore, conversions obtained in this study could be directly related to chemical kinetics, as the microreactor design ensured that mixing effects are negligible.

The bisalkylation reaction was first investigated because it could be decoupled from the first reaction step. Upon reacting **1** with **3**, two product peaks were observed by HPLC, corresponding to two diastereomers of **5** (resulting from using a racemic mixture of **1**). This was confirmed by performing an experiment with an optically pure enantiomer of **1** and observing only one bisalkylation peak. No major peak corresponding to **6** was observed, indicating good selectivity of the bisalkylation towards regioisomer **5**.

The order of the reaction of the formation of **5** from **1** and **3** was determined by analyzing the results of varying reagent concentrations (Figure 2), as well as fitting all obtained data points to a rate model of first order in each of **1** (referred to as SO in the equations) and **3** (designated as Pr), plotting  $(1)/([\text{SO}]_0 - [\text{Pr}]_0) \ln [(1 - ([\text{Pr}]_0 - [\text{SO}]_0)/([\text{Pr}]))(([\text{Pr}]_0)/([\text{SO}]_0))]$  versus

time or  $(1)/([\text{Pr}] - (1)/([\text{Pr}]_0))$  versus time for data obtained with equivalent starting amounts of **1** and **3**. The mass balances of the sample analysis closed to within the aforementioned range relative to both of the reagents (**1** and **3**). The amount of initial regioisomer **4** remained unchanged (to the limit of our detection) in all samples, indicating that the rate of aminolysis of **1** by this amine is insignificant and can be disregarded in the overall rate law estimation. Additionally, no peaks corresponding to **6** or **7** have been observed in screening studies.

The initial rates of reaction were approximated by measuring the amount of product produced at the 20-s residence time (shown in Table 1), consistently showing a rate increase by a factor near 2 for every doubling of either reagent concentration. Additionally, the plot of Figure 2c fit well to a linear correlation. Combined, these results indicate that, at the evaluated conditions, the reaction is first order with respect to each of **1** and **3**, or following the rate law:

$$r_{\text{Bis}} = r_{\text{Bis1}} + r_{\text{Bis2}} = k_{\text{Bis1}}[\text{SO}][\text{Pr}] + k_{\text{Bis2}}[\text{SO}][\text{Pr}] = (k_{\text{Bis1}} + k_{\text{Bis2}})[\text{SO}][\text{Pr}] \quad (1)$$

where Pr is desired product **3** and  $k_{\text{Bis1}}$  and  $k_{\text{Bis2}}$  represent the rate constants of bisalkylation to form the two diastereomers of **5**.

The Arrhenius dependence was performed by varying the temperature between 140 and 180 °C, at a residence time of 60 s and concentrations of **1** and **3** of 0.05 M each. Figure 3 shows the temperature dependences of **5** formation as plots of  $\ln(k_{\text{Bis1}})$  and  $\ln(k_{\text{Bis2}})$  vs  $1/T$ . The Arrhenius parameters were determined to be:

$$k_{\text{Bis1}} = e^{(-2.66 \pm 0.65) - \left(\frac{8.4 \pm 2.4 \text{ kJ/mol}}{RT}\right)} k_{\text{Bis1,453K}} = (7.5 \pm 6.9) \times 10^{-3} \text{ M}^{-1} \text{ s}^{-1} \quad (2)$$

$$k_{\text{Bis2}} = e^{(-1.89 \pm 0.62) - \left(\frac{12.0 \pm 2.2 \text{ kJ/mol}}{RT}\right)} k_{\text{Bis2,453K}} = (6.2 \pm 5.3) \times 10^{-3} \text{ M}^{-1} \text{ s}^{-1} \quad (3)$$

The observed rate constant data showed good agreement with the experimental results obtained in our previous work.<sup>18</sup> The

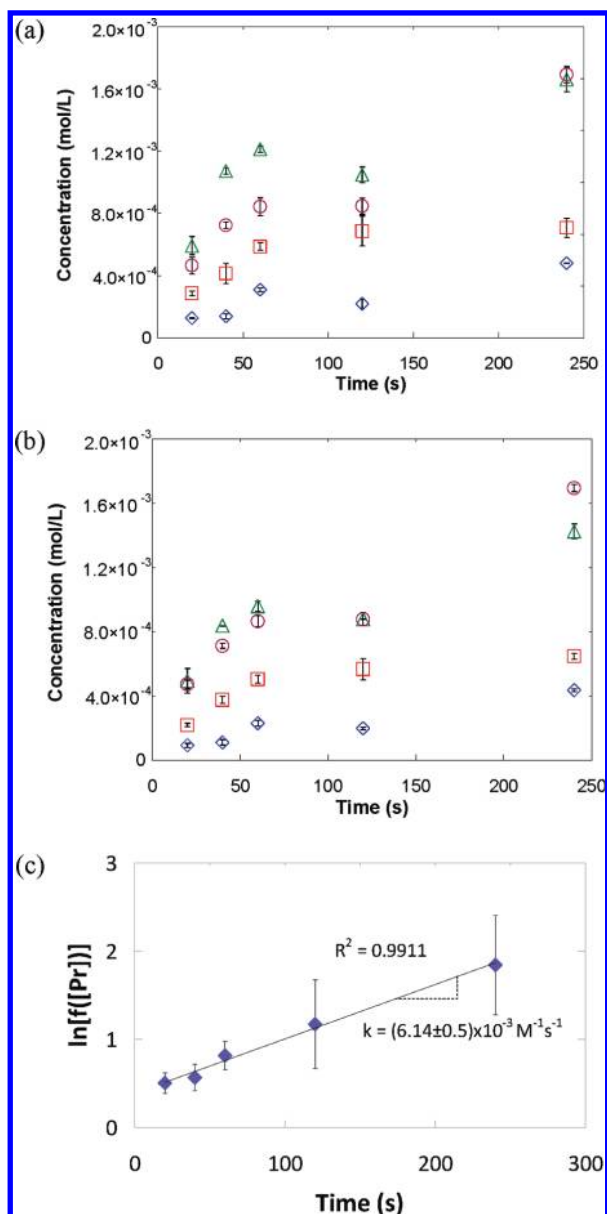


**Figure 2.** Bisalkylation reaction order determination through evolution of concentrations of the two diastereomers of product 5 [(a) and (b)] ( $\diamond$ : initial concentrations of 1 and of 3 of 0.025 M each;  $\square$ : initial concentration of 1 of 0.025 M and of 3 of 0.050 M;  $\Delta$ : initial concentration of 1 of 0.025 M and of 3 of 0.10 M;  $\circ$ : initial concentrations of 1 and of 3 of 0.050 M each); (c) plot of all reaction data points as a natural logarithm function of concentration of 3 vs time.

**Table 1.** Initial reaction rates of formation of the two diastereomers of 5 in the experiments in Figure 2 (a) and (b) (right and left sections of cells, respectively), given as  $10^{-6} \text{ mol L}^{-1} \text{ s}^{-1}$

		concentration of 1	
		0.025 M	0.05 M
concentration of 3	0.025 M	6.37; 4.56	
	0.050 M	14.3; 10.9	29.6; 23.6
	0.10 M	32.4; 23.6	

confidence intervals in the above equations were determined using the error propagation method<sup>21</sup> (Supporting Information).

**2.3. Kinetic Evaluation of Primary Aminolysis.** Having the information regarding the kinetics of bisalkylation enabled

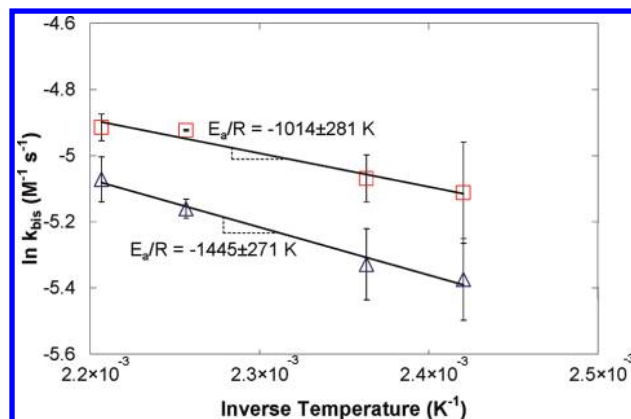


**Figure 3.** Arrhenius correlation between temperature and rate constants of bisalkylation ( $\square$  and  $\Delta$ : the two bisalkylation diastereomer products).

us to account for the rate of consumption of 1 due to that reaction in addition to the primary aminolysis. At the explored conditions, the ratios of the two bisalkylation products were nearly identical to the ratios obtained at the same temperature during the bisalkylation kinetics investigation, and no quantifiable amounts of bisalkylation products 6 or 7 were observed by HPLC. This indicates that the side product 4 does not participate in the bisalkylation reaction to a significant extent, thus allowing us to discount the consumption of 1 by that reaction route.

The orders of the reaction of the formation of 3 and 4 from 1 and 2 were determined by analyzing the results of varying the reagent concentrations (Figure 4), as well as fitting all obtained data points to a rate model of first order in each of 1 and 2 (referred to as AI in the equations), plotting  $(1)/([AI]_0 - [SO]_0) \ln \left[ \frac{1 + ([AI]_0 - [SO]_0)/([SO])}{([SO]_0)/([AI]_0)} \right]$  versus time. On the basis of the above discussion, the sum total of the bisalkylation products was attributed to the reaction of 3 with 1; thus, the produced concentrations of 5 were added to that of 3 for the calculation of the rate constants.

The initial rates of reaction were approximated by measuring the amount of product produced at the 20-s residence time (shown in Table 2), consistently showing a rate increase by a factor near 2 for every doubling of either reagent concentration. Additionally, the plot of Figure 4c fits very well to a linear correlation. Combined, these results indicate that, at the evaluated conditions, both bisalkylation reactions are first order each with respect to 1 and 2, or following the rate law:

$$r_i = k_i [SO][AI] \quad (4)$$

where  $r_i$  represents the rate of formation of 3 ( $k_1$ ) or of 4 ( $k_2$ ). Therefore, the rates of formation of the product 3 and of consumptions of 1 and 2 are expressed as follows:

$$r_{Pr} = k_1 [SO][AI] - (k_{Bis1} + k_{Bis2}) [SO][Pr] \quad (5)$$

(21) Young, H. D. *Statistical Treatment of Experimental Data*; McGraw-Hill: New York, 1962.



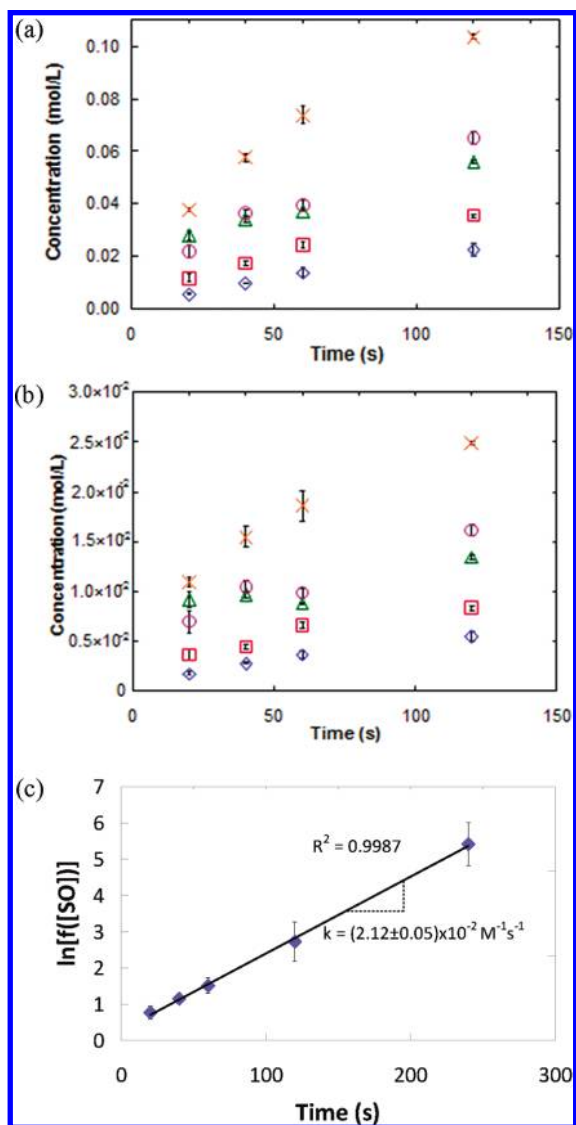


**Figure 4.** Aminolysis reaction order determination of (a) product 3 and (b) regioisomer 4 by varying concentration ( $\diamond$ : initial concentrations of 1 and 2 of 0.10 and 0.12 M, respectively;  $\square$ : initial concentrations of 1 and 2 of 0.10 and 0.24 M, respectively;  $\Delta$ : initial concentrations of 1 and 2 of 0.10 and 0.48 M, respectively;  $\circ$ : initial concentrations of 1 and 2 of 0.20 and 0.24 M, respectively;  $\times$ : initial concentrations of 1 and 2 of 0.20 and 0.48 M, respectively); (c) plot of all reaction data points as a natural logarithm function of concentration of 1 vs time.

**Table 2.** Initial reaction rates of formation of 3 and 4 in the experiments in Figure 4 a and b (right and left sections of cells, respectively), given as  $10^{-4} \text{ mol L}^{-1} \text{ s}^{-1}$

		concentration of 1	
		0.10 M	0.20 M
concentration of 2	0.12 M	2.86; 8.67	
	0.24 M	5.85; 18.3	11.0; 34.9
	0.48 M	12.4; 20.1	21.9; 66.5

$$r_{\text{SO}} = -(k_1 + k_2)[\text{SO}][\text{AI}] - (k_{\text{Bis1}} + k_{\text{Bis2}})[\text{SO}][\text{Pr}] \quad (6)$$

$$r_{\text{AI}} = -(k_1 + k_2)[\text{SO}][\text{AI}] \quad (7)$$

where  $k_{\text{Bis1}}$  and  $k_{\text{Bis2}}$  were defined and calculated in the previous section.

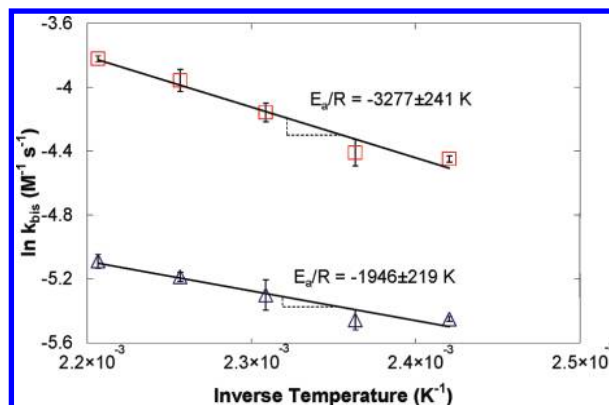


**Figure 5.** Arrhenius correlation between temperature and the rate constants of 1 aminolysis ( $\square$ : product 3;  $\Delta$ : regioisomer 4).

The Arrhenius dependence was performed by varying the temperature between 140 and 180 °C, at a residence time of 60 s and concentrations of 1 and 2 of 0.10 and 0.12 M, respectively. Figure 5 shows the temperature dependences of 3 and 4 formation as plots of  $\ln(k_1)$  and  $\ln(k_2)$  vs  $1/T$ . The Arrhenius parameters were determined to be as follows, with errors calculated by the error propagation method (Supporting Information):

$$k_1 = e^{(3.41 \pm 0.55) - \left(\frac{27.2 \pm 2.0 \text{ kJ/mol}}{RT}\right)} \quad k_{1,453\text{K}} = (2.2 \pm 1.7) \times 10^{-2} \text{ M}^{-1} \text{ s}^{-1} \quad (8)$$

$$k_2 = e^{(-0.80 \pm 0.50) - \left(\frac{16.2 \pm 1.8 \text{ kJ/mol}}{RT}\right)} \quad k_{2,453\text{K}} = (6.1 \pm 4.2) \times 10^{-3} \text{ M}^{-1} \text{ s}^{-1} \quad (9)$$

As expected on the basis of the electron properties of the amine nitrogen, which make it more reactive as a secondary amine than as a primary amine,<sup>2</sup> the activation energies of the primary alkylation are higher than those of the bisalkylation. However, the pre-exponential factors are much greater, as would be expected on the basis of the steric effects. Overall, this indicates that, while the bisalkylation is often much faster than the first alkylation in similar reactions at lower temperatures, the large disparity in activation energies leads to a much better selectivity for the desired single alkylation at increased temperatures. Additionally, the slightly higher activation energy toward the desired product 3 as compared to that toward the regioisomer 4 also leads to improved selectivity for the desired product with increased temperature.

Additionally, the model can be used to provide a response surface of product yield with varying parameters such as reaction temperature, residence time, and concentrations and stoichiometric ratios of reagents. An ordinary differential equation solver on the rate expressions given in eqs 5–7 (along with the algebraic eqs 2, 3, 8, and 9 describing the Arrhenius dependences of the rate constants on temperature) was applied to generate such a surface, with Figure 6 showing some of the corresponding time-slice cross sections and demonstrating the effects of the aforementioned parameters.

Because the rate constant of formation of 3 has the strongest dependence on temperature among the calculated rate constants,

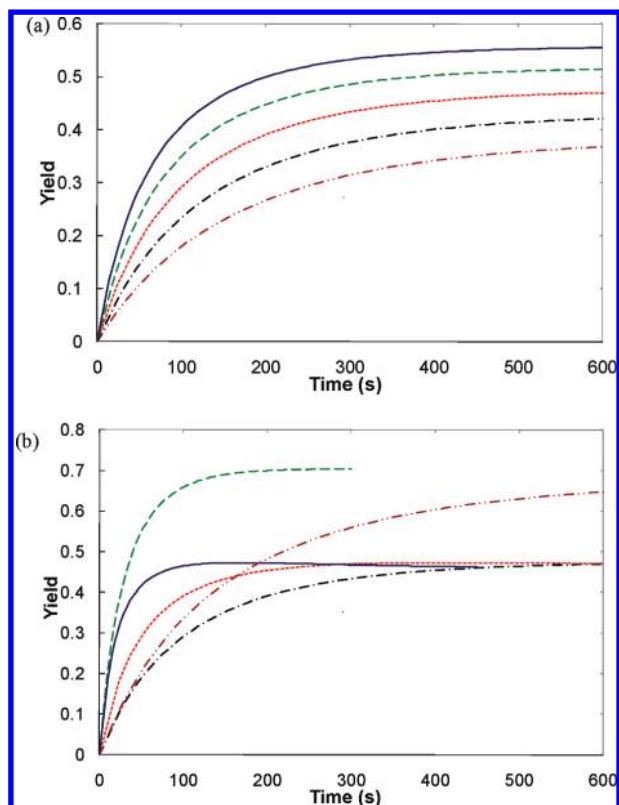


**Figure 6.** Modeled yield of **3** with time: (a) starting concentrations of 0.2 M **1** and 0.24 M **2**; blue solid line: 220 °C; green dashed line: 200 °C; red dotted line: 180 °C; black dot–dash line: 160 °C; brown dot–dot–dash line: 140 °C; (b) at 180 °C with varying initial concentrations of **1** and **2**; blue solid line: 1.0 and 1.2 M, respectively; green dashed line: 0.40 and 1.2 M, respectively; red dotted line: 0.40 and 0.48 M, respectively; black dot–dash line: 0.20 and 0.24 M, respectively; brown dot–dot–dash line: 0.10 and 0.24 M, respectively.

the model shows that higher temperatures lead to an improved overall yield in addition to a faster reaction. Indeed, we have seen that to be the case in the reaction screening study.<sup>18</sup> Additionally, the model shows that a higher excess of the amine leads to a better yield relative to the epoxide. Because the amine is often a much less expensive reagent and can also be recovered after the reaction, on scale it may be desirable to perform this reaction at very high excesses of amine to drive the highest possible product yield. If a smaller excess of amine is used, then there may be a maximum in the yield relative to time, as there may be a point at which there is sufficient product and epoxide in solution for the bisalkylation reaction to be faster than the primary product formation. Therefore, if it is desirable to use only a small excess of the amine, then it is important to know when the yield maximum occurs and to stop the reaction at that point, rather than proceeding to full conversion of the epoxide, as this would only cause loss of product. This underscores the significance of understanding the reaction kinetics.

**Table 3.** Comparison of key properties of the micro- and mesoreactors

	volume (mL)	cross section (mm <sup>2</sup> )	length (mm)	flow rate (mL/min)	velocity (mm/s)	<i>Re</i>	<b>D</b> (m <sup>2</sup> /s)	<i>Pe</i> <sub>Ax</sub>	<i>De</i>	yield (%)
microreactor	0.120	0.160 (square)	750	0.03–0.36	3.12–37.5	0.9–10.8	9.8 × 10 <sup>-6</sup> – 1.4 × 10 <sup>-3</sup>	600–100	0.16–2.4	59–69 <sup>18</sup>
mesoreactor	12.5	7.1 (circular)	1760	6.24	14.6	27.8	9.8 × 10 <sup>-3</sup>	2.6	4.2	78.0–78.2

The utility of microreactors for kinetic studies was evident in this study. The setup enabled, with a single preparation of two reagent solutions, to scan up to 35 sets of conditions (concentrations, temperatures, and residence times) with samples in triplicate, generating over 100 data points within one 8-h period. Additionally, this procedure minimizes reactant use and waste, as only 0.5–2 g of each reagent was necessary for such an experiment set, and of the total of 30 mL of reaction solution (including solvent for concentration control), fully 10 mL was used directly as HPLC samples.

**2.4. Reaction Scale-Up.** To demonstrate the applicability of the microreactor-obtained kinetic knowledge, the derived kinetic model for the aminolysis of **1** with **2** was applied to scaled-up flow and concentrations of reagents, using a 12.5-mL stainless-steel-tube reactor (see Experimental Section). The increased production was intended to verify that the information resulting from microscale experiments is applicable to mesoscale systems, from which performance in macroscale plants can be gauged more easily. Additionally, conditions were intentionally selected to be outside the scope of the model derivation to ascertain whether the model is consistent in a wider parameter space.

A set of conditions was selected on the basis of the derived kinetic model. As can be seen in Figure 6, the optimal yield relative to the epoxide reagent is achieved at higher temperatures and with larger excess of the amine reagent. Thus, the reaction conditions were selected as follows. The concentration of **1** was selected as 0.4 M to mimic the solubility limit for the indacaterol precursor epoxide, as discussed in our prior work.<sup>18</sup> The concentration of **2** was selected as 1.2 M, or a factor of 3 of the epoxide concentration. As any excess of similar amines is recovered downstream in similar industrial processes, this is feasible both economically and in the process setup.

Using the conditions described above and the derived kinetic model, 99% conversion of **1** is expected at 110 s, resulting in 76.0% ± 4.9% yield (see Supporting Information for error propagation calculations). However, these values are obtained assuming plug flow, which was reasonable in the microreactor. Table 3 compares the key parameters of the micro- and mesoreactors, including important nondimensional fluid dynamics properties, which are discussed below.

The axial dispersion Péclet number is calculated as follows:

$$Pe_{Ax} = \frac{uL}{D} \quad (10)$$

with *L* being the length of the tube, *u* being the linear velocity, and **D** being the dispersion coefficient, given by the following equation:<sup>22</sup>

$$D = \mathcal{D} + \frac{u^2 d^2}{192 \mathcal{D}} \quad (11)$$

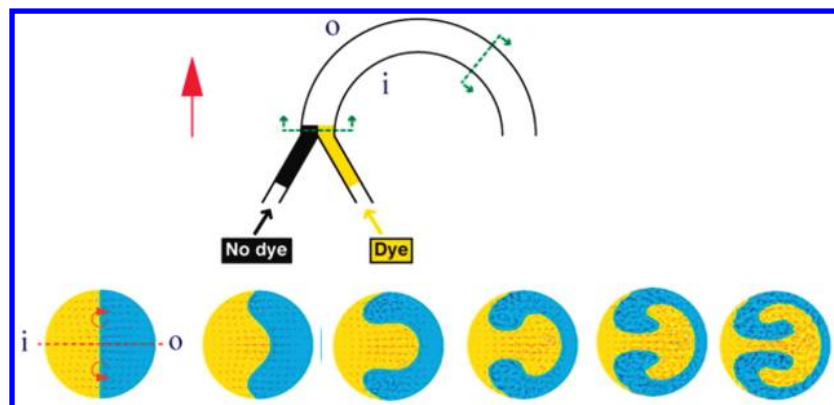


**Figure 7.** Cartoon of the effect of Dean flow in a curved cylindrical tube on two incoming sections of fluid; the bottom array demonstrates the effect of increasing Dean number (from left to right). Adapted from Sudarsan and Ugaz.<sup>24</sup>

where  $\mathcal{D}$  is the diffusion coefficient,  $u$  is the linear velocity, and  $d$  is the equivalent diameter. A diffusion coefficient  $\mathcal{D}$  of  $10^{-9}$  m<sup>2</sup>/s was used (while exact values for the starting materials in ethanol were not available, compounds similar in size and functional groups displayed diffusivities of this scale<sup>23</sup>). The axial dispersion Péclet number  $Pe_{Ax}$  for the microreactor indicates little deviation from plug flow. As the larger-scale reactor has a fairly large inner diameter and as flow is fairly rapid, dispersion is expected to play a large role. The first moment of residence time distribution  $\mathbf{E}$  was calculated on the basis of the dispersion coefficient  $\mathbf{D}$  calculated above. Because the active reactor section is a length of channel that is directly and seamlessly connected to identical channels in the cooled reactor section at both the inlet and outlet, entrance and exit effects can be neglected; thus, the reactor channel can be treated as an ‘open–open’ vessel with axial dispersion, to which the following relation applies:<sup>22</sup>

$$\mathbf{E}_t = \frac{u}{\sqrt{4\pi\mathbf{D}t}} e^{-(L-ut)^2/4\mathbf{D}t} \quad (12)$$

Conversion in a reactor with dispersion is given as:<sup>22</sup>

$$\bar{X}_{out} = \int_0^\infty X_{A, PFR}(t) \mathbf{E}(t) dt \quad (13)$$

Performing this calculation on the kinetic model results in a yield of the product **3** of  $73.0\% \pm 4.7\%$ , about 3.3% lower than what is expected in a plug-flow reactor, although the confidence intervals overlap with those of yield without dispersion. Additionally, because it is a curved tube, dispersion is expected to be reduced due to Dean flow. In Dean flow, fluid is transported from the inner to the outer wall due to the balance of forces on the fluid caused by the curvature of the tube, as shown in Figure 7, adapted from Sudarsan and Ugaz.<sup>24</sup> This transport of fluid across the cross section greatly increases radial mixing, which acts to counter the effects of

dispersion due to the parabolic flow profile. The Dean number  $De$  is given as:

$$De = Re \sqrt{\frac{D}{2R}} \quad (14)$$

where  $D$  is the inner diameter of the pipe and  $R$  is the curvature radius. With the Schmidt number (using properties of pure ethanol) calculated to be 1500, the value of  $De^2Sc$  is 26500, in which regime the effective dispersion is expected to be about 20% of the calculated value,<sup>25</sup> making it more similar to plug flow. Thus, the expected yield of **3** would be  $75.4\% \pm 4.9\%$ . Overall, the yields with and without dispersion and Dean flow have overlapping confidence intervals; thus, it is not expected to be able to determine experimentally the effect of dispersion on this system.

This reaction was performed by flowing a total of 163 mL (13 residence volumes) of solution through the reactor, taking a total of less than 30 min. Samples were taken at 3, 8, and 12 residence volumes. Each sample showed 100% conversion (no significant amount of **1** was detected), and the yield of the desired product **3** was between 78.0 and 78.2% (by HPLC, nonisolated) for all three samples, which is within the confidence intervals of the value predicted by the model. Overall, the mesoscale setup reproducibly synthesized 9.2 g of desired product **3** in 30 min, with a higher yield than previously reported for this reaction.

### 3. Conclusion

The kinetics of epoxide aminolysis were investigated at high temperatures and pressures, using styrene oxide **1** and 2-aminoindan **2** as the reagents. The bisalkylation reactions between the desired product **3** and the epoxide were investigated individually and decoupled from the primary aminolysis kinetics. The overall reaction model for the production of the desired product was obtained, including the temperature dependence, suggesting performing this reaction at the highest possible temperatures with a large excess of the amine reagent to obtain optimal yields. This study demonstrated the utility of microreactor-

(22) Levenspiel, O. *Chemical Reaction Engineering*, 3rd ed.; Wiley: New York, 1999; p 32.

(23) Myint, S.; Daud, W.; Mohamad, A.; Kadhum, A. *J. Am. Oil Chem. Soc.* **1996**, *73* (5), 603–610.

(24) Sudarsan, A. P.; Ugaz, V. M. *Proc. Natl. Acad. Sci. U.S.A.* **2006**, *103* (19), 7228–7233.

(25) Johnson, M.; Kamm, R. D. *J. Fluid Mech.* **1986**, *172*, 329–345.



based flow systems for kinetic study to enable greater understanding of a reaction and subsequent optimization of the synthesis. A robust high-pressure, high-temperature microreactor with very rapid thermal control enabled highly efficient reaction and kinetics evaluations, greatly reducing experiment preparation time relative to batch screening and minimizing reagent consumption. A total of less than 5 g each of styrene oxide **1** and 2-aminoindan **2** were necessary to perform a full multistep kinetic study, with the ability to complete up to 35 reactions in a wide range of concentrations, residence times, and temperatures in a single workday with only a single preparation of two reagent solutions per day. The determined kinetic parameters indicated that the activation energy of the formation of the desired product **3** is higher than those for the formation of regioisomers and for the bisalkylation reactions. This results in the fortuitous effect that conditions that lead to a faster reaction and higher conversion (higher temperature) also improve reaction selectivity towards the desired product. A scale-up of this reaction was performed in a 12.5-mL steel tube mesoreactor, for which dispersion was calculated and shown to have very little effect. Synthesis of 9 g of desired product **3** was achieved in 30 min, with 100% conversion and 78% yield (by HPLC, nonisolated), in good agreement with predictions from the kinetic models, thus applying attained reaction understanding to gain significant improvement in product yield over previously reported procedures.

## 4. Experimental Section

**4.1. Microreactor Fabrication and Setup.** The setup to perform the kinetics determination was identical to that used in our previous work.<sup>18</sup> In brief, a silicon microreactor was fabricated by deep reactive ion etching to form a square cross-section channel (400  $\mu\text{m}$  on the side), with a reactive volume of 120  $\mu\text{L}$ . The inlet and outlet section of the reactor was compressed in an aluminum fluidic interface chuck with Kalrez O-rings (Z1028 FFKM, size 005, Marco Rubber) and was thermally isolated from the reactive area to allow it to be cooled. A thermocouple was inserted into the heating interface of the reactive zone at a depth 0.5 mm below the aluminum surface in contact with the silicon device (with a 1-mm-thick graphite liner between the aluminum and the silicon). To confirm the thermal separation, finite element modeling was performed (Comsol Multiphysics 3.2).

Inlet tubing was connected to three 8-mL high-pressure stainless steel syringes (702267, Harvard Apparatus), which were independently driven by three syringe pumps (PHD 2200, Harvard Apparatus). The outlet tubing was connected to a backpressure regulator, either 250 psi (U-608, Upchurch) or 500 psi (U-609, Upchurch). A standard PID controller (CN742, Omega) was used to regulate temperature using two 35-W cartridge heaters (CSS-01235/120 V, Omega). See Supporting Information for heat transfer analysis.

**4.2. Microreactor Protocols for Epoxide Aminolysis Kinetics.** Two solutions in ethanol were prepared, one of the desired epoxide (**1** at 1 M or **3** at 0.25 M) with naphthalene (internal standard, 10 mol %) and the other of **2** (1.2 or 0.25 M), and placed in 8-mL high-pressure

stainless steel syringes. A third 8-mL syringe was filled with pure ethanol. The reagent streams were pumped through the microreactor at 250-psi backpressure at different flow rates to attain desired concentrations of the two reagents and reaction times. Temperature was varied from 140 to 180  $^{\circ}\text{C}$ . In general, five microreactor volumes ( $5 \times 120 \mu\text{L}$ ) were allowed to pass through the outlet after each change in conditions to achieve steady state before samples were taken for quantitative analysis. At each set of conditions, samples were collected in triplicate.

**4.3. Microreactor Synthesis of **3**.** To perform the evaluation of the bisalkylation kinetics, it was necessary to synthesize **3**, which was performed using the microreactor system. Two syringes were loaded with 2 M **1** and 2.4 M **2**, respectively, each in ethanol (resulting in 1 and 1.2 M of **1** and **2**, respectively, in the reactor). The solutions were then flowed into the microreactor at 225  $^{\circ}\text{C}$  and 500 psi with a residence time of 4 min, and the outflow was collected. Upon cooling to room temperature and solvent evaporation, an off-white crystalline solid was formed. <sup>1</sup>H NMR and HPLC confirmed it to be the desired product **3** with 97% purity (the balance was regioisomer **4**). This was deemed acceptable for the kinetic study and was used without further purification.

**4.4. Scaled-Up Synthesis Setup.** The scale-up was performed in a 6-ft-long (1.8 m), 316 stainless-steel smooth-bore seamless tube, 1/4" o.d., 0.12" i.d. (3 mm) (McMaster, 89785K52), coiled at a 10-cm turn diameter, with 171 cm (12.5 mL) submerged in a 2-L bath of high-temperature silicone oil 200.50 (Hart Scientific, 5014). The reactor was connected on both ends to 1/16" stainless-steel tubing by stainless-steel reducing swaging unions (McMaster, 5182K242). At the outlet end, 30 cm of narrow tubing connected the reactor to the 500-psi backpressure regulator used previously, which flowed out to a collection bottle. At the inlet end, 20 cm of narrow tubing connected to the reactor a compression-packaged two-stream silicon micromixer<sup>26</sup> (see Supporting Information on micromixer fabrication details). The two inlets of the micromixer were fed by HPLC single-piston pumps (Rainin Dynamax SO-200). The oil bath was placed on a stirplate with a 10-cm long magnetic stirbar and stirred at 200 rpm. Heating was achieved by an immersion heater controlled by a J-KEM Scientific two-channel controller, monitored by a K-type thermocouple probe. The outer walls of the oil bath were covered with 1"-thick fiberglass rope for thermal insulation. The reaction was performed at 220  $^{\circ}\text{C}$ , at which temperature, placing another thermocouple at different positions within the bath (including by the bath wall vs center, at the bottom vs near the surface) showed a maximum temperature difference of 0.2  $^{\circ}\text{C}$ . The two pumped solutions were **1** (0.8 M) with 10 mol % naphthalene and **2** (2.4 M) to result in a reaction stream of **1** and **2** at 0.4 and 1.2 M, respectively.

**4.5. Analytical.** HPLC quantitative analysis was performed on an Agilent 1200 series LC/MS using either an Eclipse XDB-C18 or a Zorbax Eclipse Plus C18 reverse phase column, a

(26) Zaborenko, N.; Murphy, E. R.; Kralj, J. G.; Jensen, K. F. *Ind. Eng. Chem. Res.* **2010**, *49* (9), 4132–4139.



methanol/water mobile phase, and a 254- or 210-nm wavelength detector. All reported yields were nonisolated, attained by HPLC based on normalization of response factors using naphthalene as an internal standard. Nearly all samples had mass balances between 96% and 102%, which was judged acceptable on the basis of HPLC variability. The small number of samples with mass balances outside this range were not considered in the kinetics evaluation.

### **Acknowledgment**

This work was supported by the Novartis-MIT Center for Continuous Manufacturing. We thank the members of this team

for advice, in particular, Gerhard Penn, Berthold Schenkel, Oljan Repic, Thierry Schlama, Mike Girgis, Lukas Padeste, and Felix Kollmer.

### **Supporting Information Available**

Heat transfer modeling and calculations of the microreactor; layout and microfabrication of the micromixer; error propagation derivations for kinetic rate constants and yield; dispersion calculations of the steel mesoreactor. This material is available free of charge via the Internet at <http://pubs.acs.org>.

Received for review September 16, 2010.

OP100252M